Science Advances

AAAS

advances.sciencemag.org/cgi/content/full/3/2/e1600396/DC1

Supplementary Materials for

Revealing physical interaction networks from statistics of collective dynamics

Mor Nitzan, Jose Casadiego, Marc Timme

Published 10 February 2017, *Sci. Adv.* **3**, e1600396 (2017)
DOI: 10.1126/sciadv.1600396

This PDF file includes:

- note S1. Details of the derivation of invariant-based reconstruction.
- note S2. Error estimates for observables from sampled invariant density.
- note S3. Reconstruction evaluation.
- note S4. Moderate influence of link density.
- note S5. Reconstructing homogeneous and heterogeneous networks.
- note S6. Reconstruction of systems near fixed points.
- note S7. Reconstruction of chaotic systems.
- note S8. Performance compared with available standard baselines.
- note S9. Distinguishing activating from inhibiting interactions.
- note S10. The effect of missing information.
- note S11. Model descriptions.
- note S12. The effect of various driving conditions on reconstruction quality.
- note S13. Compressed sensing.
- fig. S1. Approximating the center of mass of invariant densities by the sample mean.
- fig. S2. Sparser networks require fewer experiments for robust reconstruction.
- fig. S3. Reconstruction is robust across network topologies.
- fig. S4. The quality of reconstruction increases with the number of experiments for a network of genetic regulators.
- fig. S5. Reconstruction of a network of Rössler oscillators exhibiting chaotic dynamics.
- fig. S6. Comparison of reconstruction quality across different approaches.
- fig. S7. Comparison of reconstruction quality against transfer entropy.

- fig. S8. Separate reconstruction of activating and inhibiting interactions enhances the quality of reconstruction.
- fig. S9. Quality of reconstruction (AUC score) decreases gradually with the fraction of hidden units in the network.
- fig. S10. Quality of reconstruction increases as driving signals overcome noise and finite sampling effects.
- References (*48–50*)

1 Details of the derivation of invariant-based reconstruction

Consider networks of units $i \in \{1, \ldots, N\}$ represented by D-dimensional state variables $x_i(t) \in \mathbb{R}^D$ evolving in time t according to

$$\dot{x}_{i,d}(t) = F_{i,d}(x(t)) + \xi_{i,d}(t) \tag{1}$$

Here $d \in \{1, \ldots, D\}$, $x(t) = (x_1(t), \ldots, x_N(t)) \in \mathbb{R}^{ND}$ is the state vector of the entire network, $\dot{x}_{i,d}(t) \equiv \frac{d}{dt} x_{i,d}(t)$ denotes the temporal derivative of the variable $x_{i,d}(t)$, and $\xi_{i,d}(t)$ represents noise with zero average.

Driving the system with signals $I_{i,d}^{(m)}$ yields

$$\dot{x}_{i,d}^{(m)} = F_{i,d}(x^{(m)}) + I_{i,d}^{(m)} + \xi_{i,d}^{(m)} \tag{2}$$

where $I_{i,d}^{(0)} \equiv 0$ for all i and d, and $m \in \{1, \ldots, M\}$. We consider an ND-dimensional vector observable based on long-term averaging of the dynamics, specifically, the center of mass of the vector $x^{(m)}$, $z^{(m)} = \langle x^{(m)} \rangle_\rho$, where ρ is an invariant density generated by the trajectories of the system.

If the recorded state space points sample this density well, the center of mass can be approximated by the temporal average $z^{(m)} = \langle x^{(m)}(t) \rangle_{t \in T}$. Here T is the set of time points at which the data are recorded. These data may be available without known temporal order, have been recorded at varying sampling intervals and even come from several experiments under the same conditions. Furthermore, different units of the same system may in principle be recorded separately and at different times.

Expanding equation (2) relative to $z^{(0)}$ up to first order yields

$$\dot{x}_{i,d}^{(m)} \approx F_{i,d}(z^{(0)}) + \sum_{j=1}^{N} \sum_{k=1}^{D} \left. \frac{\partial F_{i,d}}{\partial x_{j,k}} \right|_{z^{(0)}} (x_{j,k}^{(m)} - z_{j,k}^{(0)}) + I_{i,d}^{(m)} + \xi_{i,d}^{(m)} \tag{3}$$

This approximation is justified as long as higher orders of the term $(x_{j,k}^{(m)} - z_{j,k}^{(0)})$ decay sufficiently fast. Thus either the activity patterns of the nodes in the network are sufficiently close to the center of mass of the unperturbed invariant density or $F_{i,d}$ deviates sufficiently slowly beyond its first order approximation.

Now, averaging over the measurement domain T

$$\dot{z_{i,d}}^{(m)} \approx F_{i,d}(z^{(0)}) + \sum_{j=1}^{N}\sum_{k=1}^{D} \frac{\partial F_{i,d}}{\partial x_{j,k}}\Big|_{z^{(0)}} (z_{j,k}^{(m)} - z_{j,k}^{(0)}) + \bar{I}_{i,d}^{(m)} \tag{4}$$

where $\bar{I}_{i,d}^{(m)} := \langle I_{i,d}^{(m)} \rangle_{t\in T}$ are the temporal averages of the driving signals.

We notice that

$$\dot{z_{i,d}}^{(0)} \approx F_{i,d}(z^{(0)}) \tag{5}$$

Plugging in the expression for $F_{i,d}(z^{(0)})$ from equation (5), equation (4) becomes

$$\dot{z_{i,d}}^{(m)} - \dot{z_{i,d}}^{(0)} \approx \sum_{j=1}^{N}\sum_{k=1}^{D} J_{ij,dk}(z_{j,k}^{(m)} - z_{j,k}^{(0)}) + \bar{I}_{i,d}^{(m)} \tag{6}$$

where $J_{ij,dk} = \frac{\partial F_{i,d}}{\partial x_{j,k}}\Big|_{z^{(0)}}$ are the elements of the Jacobian $J = Df|_{z^{(0)}} \in \mathbb{R}^{ND\times ND}$.

We take $\dot{z_{i,d}}^{(m)} = \dot{z_{i,d}}^{(0)} = 0$, since the centers of mass do not change in time if the recorded points sample the density well.

This yields the first order approximation

$$-\bar{I}_{i,d} \approx \Delta z \; J_{i,d}^{\mathsf{T}} \tag{7}$$

where $I_{i,d} \in \mathbb{R}^M$ is the vector of driving signals $I_{i\,d}^{(m)}$ and $\Delta z \in \mathbb{R}^{M\times ND}$ the matrix of differences $z_{j,k}^{(m)} - z_{j,k}^{(0)}$ of the centers of mass. Sufficiently many driving-response experiments thus yield a linear set of equations (7) for each node, restricting the potential interaction networks

estimated by J. Here $J_{ij,dk} \neq 0$ if the k^{th} dimension of unit j directly acts on the d^{th} dimension of i and $J_{ij,dk} = 0$ if there is no such direct interaction. Notice that since the Jacobian is evaluated at the center of mass of the unperturbed invariant density, the reconstruction approach is expected to recover the correct interactions if they consistently exist across the relevant fractions of state space which include the observed driven dynamics and the unperturbed centers of mass.

2 Error estimates for observables from sampled invariant density

The main manuscript (equation (6)) uses that the center of mass of the invariant measure is time independent and unique. For a finite number of sampling points, the center of mass will actually depend on the exact collection of sampling points realized. So the problem boils down to estimating the mean $z^{(m)} = \langle x^{(m)} \rangle_\rho$ of a distribution (here: the invariant measure ρ) by the finite sample mean $\langle x^{(m)}(t) \rangle_{t \in T} = |T|^{-1} \sum_{t \in T} x^{(m)}(t)$. We expect the variance of the sample center of mass (or, the sample mean) $\mathrm{Var}(\langle x^{(m)}(t) \rangle_{t \in T})$ to equal to $\mathrm{Var}(x^{(m)})/T$. Figure S1 confirms this view. The actual scaling yields an order of magnitude estimate for the response to driving needed to reliably distinguish experiments under different driving conditions.

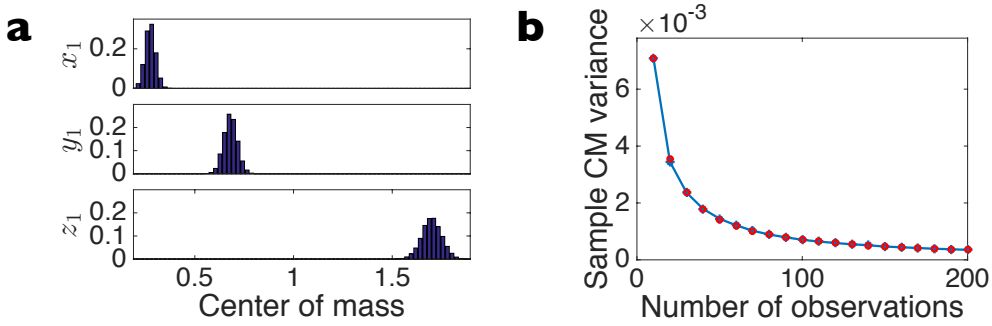

fig. S1. Approximating the center of mass of invariant densities by the sample mean. **(a)** Histograms of the center of mass of variables x, y and z of one oscillator in a network of Goodwin oscillators, computed from random samplings of 100 time points. **(b)** The variance of the sample center of mass (here shown for the variable x) (blue marks connected by a blue line) is decreasing with the number of observations T, and fits well to the variance of the variable x (estimated from 30,000 time points) over T (red circles). Data shown for random networks of $N = 50$ Goodwin oscillators with regular incoming degree 4, noise level 0.1.

3 Reconstruction evaluation

Reconstructing the network according to equation (7), considering for simplicity the case of 1-dimensional state variables, yields the entries of the estimated interaction network $J_{ij} = \left.\frac{\partial F_i}{\partial x_j}\right|_{z^{(0)}}$. The values $|J_{ij}|$ induce a ranking of all potential interactions. In order to evaluate the consistency between this reconstructed ranking and the original network, we use the notion of a receiver operating characteristic (ROC) curve. A ROC curve illustrates the performance of a binary classifier by presenting the tradeoff between the true positive rate (fraction of true positives out of the total actual positives) and the false positive rate (fraction of false positives out of the total actual negatives). An example of a ROC curve for the invariant-based reconstruction of a Goodwin oscillator network is shown in fig. S2b in the main text.

The ROC curve, in our case, can be interpreted as follows; given a ranked list of potential edges (ordered node pairs), they are gradually chosen as existing edges according to their rank. If the chosen potential edge corresponds to a real edge in the original network, the true positive

count increases by 1. Otherwise, the false positive count increases by 1. If all existing edges in the network are ranked highest in the reconstructed network, the ROC curve will be plotted as a step function, rising to true positive rate of 1 while the false positive rate is kept at 0. In general, the ROC curve will saturate more quickly as more highly ranked potential edges are within the set of actual existing edges in the original network. The quality of reconstruction can therefore be evaluated by the area under the ROC curve (AUC), which measures, in a parameter-free manner, the consistency between the reconstructed and the original network.

4 Moderate influence of link density

In the main manuscript, we studied a range of systems and systematically evaluated the influence of noise and network size on reconstruction quality. Here we highlight that reconstruction is also possible across a range of average degrees, illustrated for random networks of N=50 Goodwin oscillators with a number of incoming edges ranging from 1 to 10. The lower the degree, the lower the number of required driving response experiments (fig. S2) for high quality reconstruction.

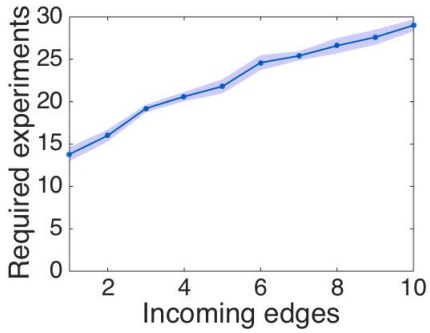

fig. S2. Sparser networks require fewer experiments for robust reconstruction. The number of experiments required for high quality reconstruction (here AUC > 0.95) grows roughly linearly with the number of incoming edges to each unit in the network. Results are shown for random networks of $N = 50$ Goodwin oscillators , number of sampled time points is 100; shading indicates standard deviation across ensembles of network realizations.

5 Reconstructing homogeneous and heterogeneous networks

The invariants-based reconstruction approach is robust for various network topologies, including homogeneous and heterogeneous structures, as shown in fig. S3 for regular, binomial and scale-free networks. Here we use least-squares solution to equation (7), in order for the reconstruction to not be biased by the sparsity of the solution, which is changing across the different topologies.

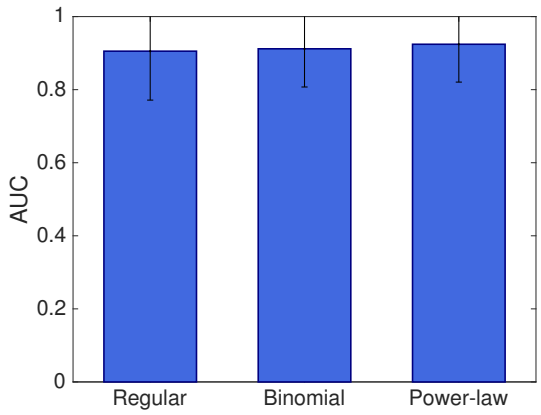

fig. S3. Reconstruction is robust across network topologies. The quality of reconstruction (AUC score) for networks with regular (each node is connected to 4 other nodes), binomial (mean degree 4, standard deviation 1) and power-law (exponent value 2.5) degree distributions. The respective mean AUC scores are 0.905, 0.912, 0.924 and their standard deviations are 0.134, 0.105, 0.104, respectively. Results are shown for random networks of $N = 40$ Goodwin oscillators, noise level 0.1, number of experiments 40, number of sampled time points 100; error bars indicate standard deviation across ensembles of network realizations.

In addition, the invariants-based approach is robust for heterogeneous coupling strengths between the network's units. When randomly sampling coupling strengths from a uniform distribution with constant lower bound 0, and varying upper bound (1,2,3,4 and 5), no significant changes in reconstruction AUC score were found (mean AUC score 0.963 across ensembles of network realizations for the five different upper bound values, standard deviation 0.017). Results were obtained for random regular (incoming degree 4) networks of $N = 40$ Goodwin

oscillators (noise level 0.1, number of experiments 20, number of sampled time points 100).

6 Reconstruction of systems near fixed points

Our reconstruction approach can be used to reconstruct the topology of networks underlying noisy dynamic processes found near fixed points. For example, we consider a biological network of transcription factor regulators, including both activators and repressors (equations (11)-(13)), whose collective dynamics is near a fixed point. Reconstruction is robust, both for the noiseless and noisy systems (fig. S4).

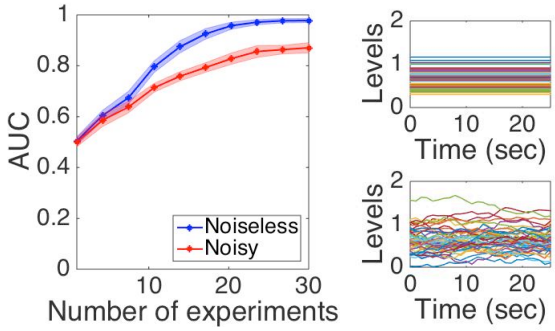

fig. S4. The quality of reconstruction increases with the number of experiments for a network of genetic regulators. Reconstruction quality (AUC score) is higher for noiseless systems (blue curve, dynamics shown on top right panel) than for noisy systems (red curve, dynamics shown on bottom right panel). Results are shown for a Erdős Rényi random network of $N = 50$ genetic regulators, with edge probability $p = 0.01$. A genetic regulator is chosen to be either an activator or a repressor with equal probability. Noise level for noisy case is 0.05, number of sampled time points is 100; shading indicates standard deviation across ensembles of network realizations.

7 Reconstruction of chaotic systems

Reconstruction can be achieved using our approach as long as the temporal trajectories of the system (after potential transients) exhibit collective dynamics that generate a defined statistics of points in state space. This means that the approach is suitable for systems exhibiting different

types of dynamics, including chaotic collective dynamics. We demonstrate this on a network of Rössler oscillators (equation (10)), whose reconstruction is robust with increasing quality as a function of the number of driving-response experiments (fig. S5).

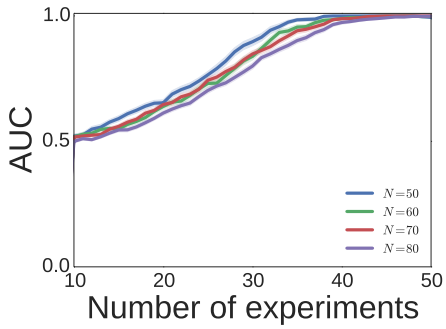

fig. S5. Reconstruction of a network of Rössler oscillators exhibiting chaotic dynamics. The quality of reconstruction (AUC score) increases with the number of driving-response experiments of a network of Rössler oscillators. Results are shown for random networks of $N \in \{50, 60, 70, 80\}$ oscillators with 10 incoming connections per node. Number of sampled time points is 6000; shading indicates standard deviation across ensembles of network realizations.

8 Performance compared with available standard baselines

Here we evaluate the results of the invariants-based reconstruction approach relative to other available standard reconstruction methods. To the best of our knowledge, a method capable of inferring physical interaction networks given asynchronous, low-resolution, temporally disordered measurements, with no prior knowledge of the system's model, does not exist to date. Therefore, we have compared our invariants-based reconstruction results to heuristic statistical baselines, specifically, measures of mutual information, correlation and transfer entropy between the activity patterns of every two nodes in the network, and partial correlation between the pairwise activity patterns, given the activity patterns of all other nodes in the network. Notice that while the invariants-based approach requires driving-response experiments or observations, the heuristic statistical baselines require synchronous measurements from all nodes in the network, and in addition, transfer entropy requires temporally ordered measurements.

As shown in fig. S6 and fig. S7, the invariants-based reconstruction approach significantly outperforms available reconstruction baselines. As fig. S7(b) illustrates, the invariants-based method performs better than transfer entropy, in particular for small number of sampled time points. While the gap in performance decreases for increasing sampled time points, it stays substantial (fig. S7(b), inset).

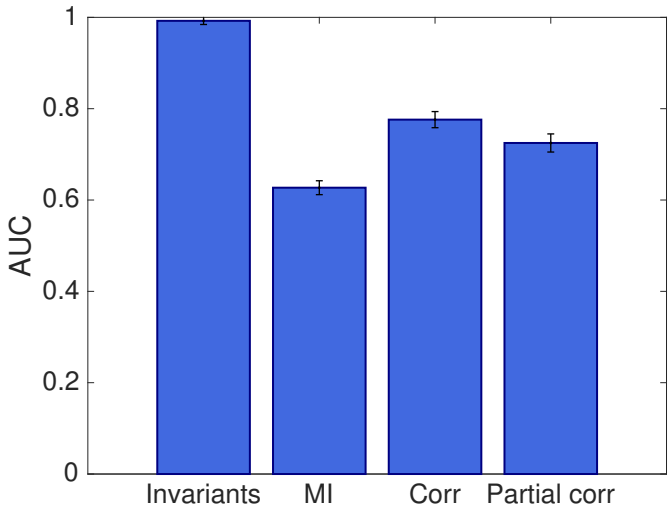

fig. S6. Comparison of reconstruction quality across different approaches. The quality of reconstruction (AUC score) given by the invariants-based approach, mutual information, correlation and partial correlation measures is shown. The respective mean AUC scores are 0.992, 0.627, 0.776, 0.725 and their standard deviations are 0.008, 0.015, 0.018, 0.020 , respectively. Reconstruction is performed on random networks of $N = 40$ Goodwin oscillators with regular incoming degree 4, noise level 0.1, number of experiments 20, number of sampled time points 100; error bars indicate standard deviation across ensembles of network realizations.

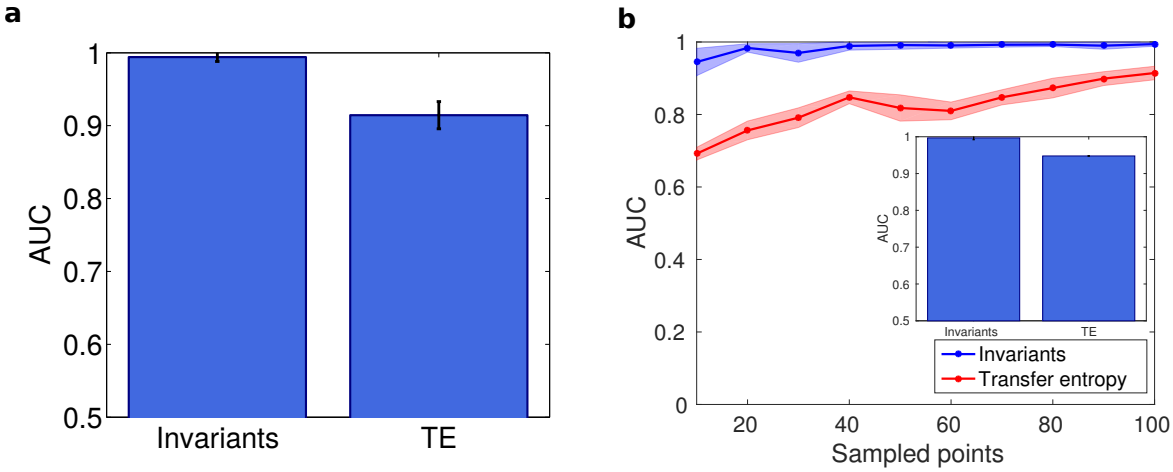

fig. S7. Comparison of reconstruction quality against transfer entropy. **(a)** The quality of reconstruction (AUC score) given by the invariants-based approach and transfer entropy. Reconstruction is performed on random networks of $N = 40$ Goodwin oscillators with regular incoming degree 4, noise level 0.1, number of experiments 20, number of sampled time points 100; error bars indicate standard deviation across ensembles of network realizations. **(b)** Quality of reconstruction for both approaches versus the number of sampled time points. The inset shows the quality of reconstruction of both methods with 1000 time points sampled.

9 Distinguishing activating from inhibiting interactions

We define an interaction from unit j to unit i to be consistently activating if for all $x \in R^N$ relevant for the system's function, $\frac{\partial F_i}{\partial x_j}\Big|_x > 0$. Analogously, we define an interaction to be consistently inhibiting if $\frac{\partial F_i}{\partial x_j}\Big|_x < 0$ for those relevant states. Therefore, one could potentially distinguish between consistently activating and consistently inhibiting interactions, in addition to distinguishing between existing and missing interactions. This distinction can be achieved by simultaneously varying two thresholds (one starting from the largest value of reconstructed J_{ij} and one from the smallest, without applying absolute value to the resulting J_{ij} entries) to produce two ROC curves, one for correctly identifying activating interactions (as opposed to inhibiting or missing interactions) and one for correctly identifying inhibiting interactions. This approach not only reveals more information regarding the functional properties of the in-

teractions in the network (in addition to their existence), it can even enhance the quality of reconstruction. The source for such enhancement is schematically exemplified in fig. S8, where separately ranking and identifying activating and inhibiting interactions would yield perfect AUC score (AUC$=1$, meaning, perfect ranking of reconstructed interactions). On the other hand, jointly ranking $|J_{ij}|$ entries to identify existence of interactions would reduce the quality of reconstruction (AUC<1), as reconstructed values of absent and repressing interactions overlap in this case.

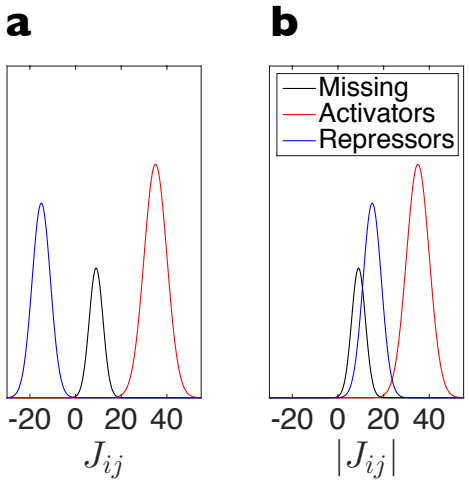

fig. S8. Separate reconstruction of activating and inhibiting interactions enhances the quality of reconstruction. (a) The schematic histograms of reconstructed network entries J_{ij} do not overlap and their ranking matches activating, repressing, and absent interactions in the original network. **(b)** Once joint reconstruction of existing and missing interactions is attempted (through $|J_{ij}|$), the missing and repressing interactions largely overlap, thus decreasing the quality of reconstruction.

10 The effect of missing information

Here we test systematically the effect of missing information (hidden units with no access to their dynamics) on the quality of reconstruction of a network of Goodwin oscillators. We find that our ability to infer the existence of interactions between observed units decreases gradually,

as the fraction of random hidden units in the network increases (fig. S9). However, adequate reconstruction is achieved even when a substantial fraction of the network is hidden. Here we use least-squares solution to equation (7), in order for the reconstruction to not be biased by the sparsity of the solution, which is changing with the number of hidden units.

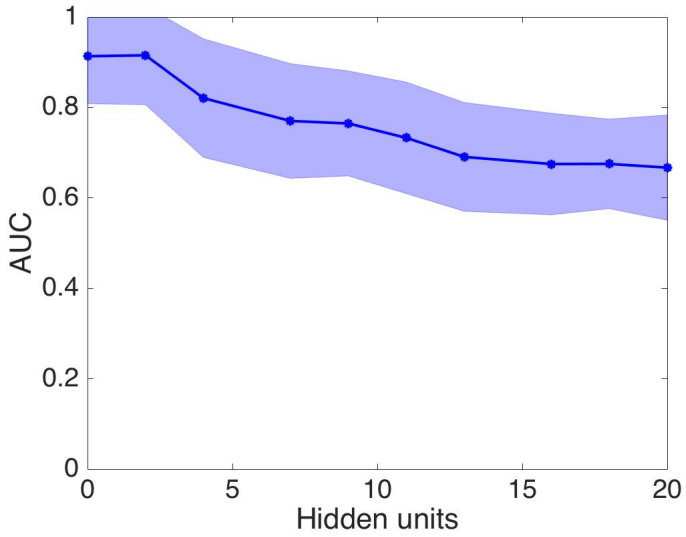

fig. S9. Quality of reconstruction (AUC score) decreases gradually with the fraction of hidden units in the network. Data shown for random networks of $N = 40$ Goodwin oscillators with regular incoming degree 4, noise level 0.1, number of experiments 40, number of sampled time points 100; shading indicates standard deviation across ensembles of network realizations.

11 Models descriptions

Circadian clock

The circadian clock in *Drosophila* is driven by two proteins, PER and TIM. The circadian oscillations in their levels result from the negative feedback exerted by a PER-TIM complex on the expression of the *per* and *tim* genes which code for the two proteins. The time evolution of the 10-variable model of the circadian clock is governed by the following rate equations (based

on (*45*))

$$\frac{dM_P}{dt} = v_{sP}\frac{K_{IP}^n}{K_{IP}^n + C_N^n} - v_{mP}\frac{M_P}{K_{mP} + M_P} - k_d M_P \tag{8a}$$

$$\frac{dP_0}{dt} = k_{sP} M_P - V_{1p}\frac{P_0}{K_{1P} + P_0} + V_{2p}\frac{P_1}{K_{2P} + P_1} - k_d P_0 \tag{8b}$$

$$\frac{dP_1}{dt} = V_{1p}\frac{P_0}{K_{1P} + P_0} - V_{2p}\frac{P_1}{K_{2P} + P_1} - V_{3p}\frac{P_1}{K_{3P} + P_1} + V_{4p}\frac{P_2}{K_{4P} + P_2} - k_d P_1 \tag{8c}$$

$$\frac{dP_2}{dt} = V_3 P\frac{P_1}{K_{3P} + P_1} - V_{4p}\frac{P_2}{K_{4P} + P_2} - k_3 P_2 T_2 + k_4 C - v_{dP}\frac{P_2}{K_{dP} + P_2} - k_d P_2 \tag{8d}$$

$$\frac{dM_T}{dt} = v_{sT}\frac{K_{IT}^n}{K_{IT}^n + C_N^n} - v_{mT}\frac{M_T}{K_{mT} + M_T} - k_d M_T \tag{8e}$$

$$\frac{dT_0}{dt} = k_{sT} M_T - V_{1T}\frac{T_0}{K_{1T} + T_0} + V_{2T}\frac{T_1}{K_{2T} + T_1} - k_d T_o \tag{8f}$$

$$\frac{dT_1}{dt} = V_{1T}\frac{T_0}{K_{1T} + T_0} - V_{2T}\frac{T_1}{K_{2T} + T_1} - V_{3T}\frac{T_1}{K_{3T} + T_1} + V_{4T}\frac{T_2}{K_{4T} + T_2} - k_d T_1 \tag{8g}$$

$$\frac{dT_2}{dt} = V_{3T}\frac{T_1}{K_{3T} + T_1} - V_{4T}\frac{T_2}{K_{4T} + T_2} - k_3 P_2 T_2 + k_4 C - V_{dT}\frac{T_2}{K_{dT} + T_2} - k_d T_2 \tag{8h}$$

$$\frac{dC}{dt} = k_3 P_2 T_2 - k_4 C - k_1 C - k_2 C_N - k_{dC} C \tag{8i}$$

$$\frac{dC_N}{dt} = k_1 C - k_2 C_N - k_{dN} C_N \tag{8j}$$

where M_T and M_P are *tim* and *per* mRNAs, respectively. T_0, T_1 and T_2 are different forms of TIM protein. P_0, P_1 and P_2 are different forms of PER protein. C and C_N are different forms of PER-TIM complex.

The total (non-conserved) quantity of PER and TIM proteins, P_t and T_t, are given by

$$P_t = P_0 + P_1 + P_2 + C + C_N \tag{9a}$$

$$T_t = T_0 + T_1 + T_2 + C + C_N \tag{9b}$$

Parameter values used for the dynamic simulations performed for the current work are based on (*45*).

Network of Rössler oscillators

We tested the reconstruction method on an N unit Rössler oscillator system (*48*), where each oscillator's dynamics is given by the three ordinary differential equations

$$\dot{x_i} = -y_i - z_i + \sum_{j=1}^{N} J_{ij} f(x_i, x_j) \tag{10a}$$

$$\dot{y_i} = x_i + a_i y_i \tag{10b}$$

$$\dot{z_i} = b_i + z_i(x_i - c_i) \tag{10c}$$

where $i \in \{1, \ldots, N\}$. a_i, b_i and c_i are local parameters (assuming in our simulations the values 0.2, 1.7 and 14 $\forall i \in \{1, \ldots, N\}$, respectively). The coupling functions were assumed to induce synchronization, $f(x_i, x_j) = x_j - x_i$ (*23*).

Transcriptional regulatory network

Consider a network of N interacting units, each represents a transcription factor protein that can affect the synthesis rate of each of its targets either positively or negatively. Unit i evolves in time according to

$$\dot{x_i} = g_{m_i} \prod_{j=1}^{N} A_{ij} g(x_i, x_j) - d_{m_i} x_i \tag{11}$$

where A is the adjacency matrix, g_{m_i} is the synthesis rate of unit i and d_{m_i} is its degradation rate.

In case unit j positively regulates unit i

$$g(x_i, x_j) = g(x_j) = \frac{{x_j}^n}{{x_j}^n + k^n} \tag{12}$$

and in case unit j negatively regulates unit i

$$g(x_i, x_j) = g(x_j) = \frac{k^n}{{x_j}^n + k^n} \tag{13}$$

where n is the hill coefficient. The parameter values used for the dynamic simulations performed for the current work are $g_{m_i} = 0.2$ sec^{-1}, $d_{m_i} = 0.07$ sec^{-1}, $k = 0.5$, $n = 1$.

12 The effect of various driving conditions on reconstruction quality

The driving signals in the experiments presented in this manuscript are distributed randomly over the different nodes in each network. As shown in fig. S10, although no fine-tuning of the driving signals is needed, driving has to be sufficiently large to outweigh the effects of noise and finite sampling in order to yield robust reconstruction.

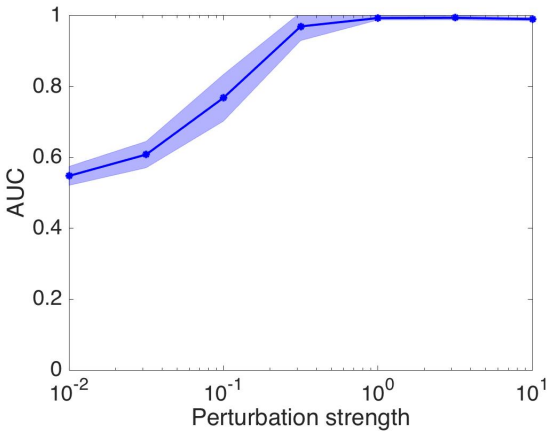

fig. S10. Quality of reconstruction increases as driving signals overcome noise and finite sampling effects. The quality of reconstruction (AUC score) increases with the amplitude of the random driving signals for a network of Goodwin oscillators. Data shown for random networks of $N = 40$ Goodwin oscillators with regular incoming degree 4, default noise level 0.1, number of experiments 20, number of sampled time points 100; shading indicates standard deviation across ensembles of network realizations.

13 Compressed sensing

In order to reconstruct a network using our approach, we need to solve a linear set of equations, as appears in equation (7) (or equation (6) in the main text)

$$-\bar{I}_i \approx \Delta z \; J_i^{\mathsf{T}} \tag{14}$$

separately for each node in the network, or equivalently, for each row of the adjacency matrix. For each such set, the number of unknowns is N, the number of nodes in the network, while the number of equations is M, the number of driving-response experiments, where for simplicity we refer to the case of 1-dimensional state variables. In many realistic natural or experimental scenarios, $M \ll N$, rendering the problem severely underdetermined. In order to restrict the space of possible network configurations that are consistent with equation (14), one possible approach would be to use prior knowledge for the structure of the network we are interested in reconstructing. Since many real-world networks are sparse (both globally and row-wise in terms of their adjacency matrix), it seems natural to use sparsity as our prior knowledge. If J_i^{T} is k-sparse ($\| \; J_i^{\mathsf{T}} \; \|_0 \leq k$) and any $2k$ columns of Δz are linearly independent, then the solution to the optimization problem

$$\begin{aligned} \text{minimize} \quad & \| \; \tilde{J}_i^{\mathsf{T}} \; \|_0 \\ \text{subject to} \quad & -\bar{I}_i = \Delta z \; \tilde{J}_i^{\mathsf{T}} \end{aligned}$$

yields J_i^{T}. This combinatorial optimization problem is NP-hard (*49*) and therefore inefficient to solve. However, recent developments in the paradigm of compressed sensing (*34–38*) show that it can be convexly approximated by the optimization problem

$$\begin{aligned} \text{minimize} \quad & \| \; \tilde{J}_i^{\mathsf{T}} \; \|_1 \\ \text{subject to} \quad & -\bar{I}_i = \Delta z \; \tilde{J}_i^{\mathsf{T}} \end{aligned} \tag{15}$$

If the measurement matrix Δz obeys the restricted isometry property with $\delta_{2k} < \sqrt{2} - 1$, then the solution to equation (15) recovers the structure J of the network (*34*). In the more realistic

case, given noisy measurement, it can be shown that if $\delta_{2k} < \sqrt{2} - 1$, then the solution to

$$\begin{aligned} &\text{minimize} \quad \| \tilde{J_i^{\mathsf{T}}} \|_1 \\ &\text{subject to} \quad \| \bar{I}_i + \Delta z \, \tilde{J_i^{\mathsf{T}}} \|_2 \leq \epsilon \end{aligned}$$

obeys

$$\| \tilde{J_i^{\mathsf{T}}} - J_i^{\mathsf{T}} \|_2 \leq C_1 \epsilon$$

for some constant C_1 (*34*). If the entries of Δz were sampled i.i.d from a Gaussian or a sub-Gaussian distribution, then with overwhelming probability, Δz would obey the restricted isometry property, provided that

$$M \geq C\dot{k} \log(N/k)$$

where C is some constant, M is the number of driving-response experiments and N is the size of the network. This means that with high probability, the entire network J can be reconstructed using a number of driving-response experiments on the order of the sparsity of incoming connections to each node, k, instead of the number of nodes in the network (*34*). These results allow us to efficiently reconstruct large networks using only a few driving-response experiments, as are often available for real systems.

Finally, given a measurement matrix Δz, we can directly evaluate its coherence properties to check whether exact reconstruction is guaranteed. Specifically, the mutual incoherence is defined by

$$\mu = \max_{i \neq j} | < \Delta z_i, \Delta z_j > | \tag{16}$$

where Δz_i denotes the i^{th} column of Δz. If

$$\mu < \frac{1}{2k - 1} \tag{17}$$

then the network structure J can be recovered exactly (*50*). In our set up, this means that the response profiles of different nodes to different perturbations should be sufficiently distinguishable, which is a reasonable requirements for real systems.